[12]V. L. Goldanskii, E. F. Makarov, I. P. Suzdalev, and I. A. Vinogradov, Zh. Eksperim. i Teor. Fiz. 54, 78 (1968) [Soviet Phys. JETP 27, 44 (1968)].
[13]M. Blume, Phys. Rev. Letters 14, 96 (1965).
[14]G. K. Wertheim, *Mössbauer Effect: Principles and Applications* (Academic, New York, 1964), p. 42.
[15]L. R. Walker, G. K. Wertheim, and V. Jaccarino, Phys. Rev. Letters 6, 98 (1961).
[16]R. V. Pound, G. B. Benedek, and R. Drever, Phys. Rev. Letters 7, 405 (1961).
[17]C. K. Edge, R. Ingalls, P. Debrunner, H. C. Drickamer, and H. Frauenfelder, Phys. Rev. 138, 729 (1965).
[18]D. N. Pipkorn, C. K. Edge, P. Debrunner, G. de Pasquali, H. G. Drickamer, and H. Frauenfelder, Phys. Rev. 135, 1604 (1964).
[19]G. K. Wertheim, V. Jaccarino, J. H. Wernick, and D. N. E. Buchanan, Phys. Rev. Letters 12, 24 (1964).

PHYSICAL REVIEW B VOLUME 2, NUMBER 7 1 OCTOBER 1970

Microwave-Optical Double Resonance of the Metastable $4f^6 5d$ Level of Eu^{2+} in the Fluorite Lattices

L. L. Chase*
Bell Telephone Laboratories, Murray Hill, New Jersey 07974
(Received 4 May 1970)

The results of an electron-spin-resonance investigation of the metastable $4f^6 5d$ level of Eu^{2+} in CaF_2, SrF_2, and BaF_2 are presented. The experiments utilized the intense fluorescence from the lowest-lying $\Gamma_8(4f^6 5d)$ level of Eu^{2+} to the $^8S_{7/2}(4f^7)$ ground state for the optical detection of resonance transitions in the excited state. The magnitudes of the Zeeman and hyperfine splittings for the excited state are consistent with the model of a large crystal-field splitting for the $5d$ electron and a considerably smaller coupling of this electron to the $4f^6$ configuration. The large average g value of 3.80 for this level can be explained by an effective exchange coupling between the $5d$ spin and the $4f^6(^7F_J)$ spin component if this coupling is comparable to the 400-cm^{-1} spin-orbit coupling parameter for the ^7F_J multiplets. The anomalous line shapes of the resonance spectrum can be interpreted on the basis of a dynamical Jahn-Teller distortion of the e_g orbital of the $5d$ electron. A singlet tunneling level associated with the Jahn-Teller effect is estimated to be at about 10 cm^{-1} above the orbital doublet Γ_8 level in both SrF_2 and CaF_2 on the basis of the line shapes observed in the resonance spectrum. Previously unidentified optical transitions to these levels have been observed by other workers, who also measured the splitting of the Γ_8 level by uniaxial strains and the strain coupling of the singlet tunneling level to the Γ_8 level. These piezo-optic data are in quantitative agreement with the model of a dynamical Jahn-Teller interaction for the observed levels. The nature of the fluorescence spectrum of Eu^{2+} in BaF_2 is basically different from that observed for Eu^{2+} in CaF_2 or SrF_2. However, an optically detected resonance spectrum identical to that of CaF_2 or SrF_2 has been observed for Eu^{2+} in BaF_2.

I. INTRODUCTION

The divalent configurations of the lanthanide elements with incomplete $4f$ shells all have strong optical absorptions in crystalline environments, beginning in the visible region of the spectrum and extending into the ultraviolet.[1] The absorption results from the electric dipole allowed $4f^n \rightarrow 4f^{n-1}5d$ transitions, which are considerably phonon broadened in crystalline spectra as a result of the large crystal-field coupling of the $5d$ electron. The electron-lattice coupling in many crystals is of such a magnitude that sharp direct transitions as well as vibrational satellites and many-phonon bands are simultaneously observed in these spectra. This property has led to much experimental activity directed toward the understanding of the electronic structure and crystalline-field interactions of the $4f^{n-1}5d$ configurations. A large portion of this work has been done using the fluorite lattices CaF_2, SrF_2, and BaF_2 as hosts for the RE^{2+} ions because most elements of this series are relatively stable in these crystals.

We report here on the results of an electron-spin-resonance (ESR) investigation of the lowest $4f^6 5d$ level of the Eu^{2+} ion in these lattices. Our work supports the model of a crystal-field splitting for the $5d$ electron, which is considerably larger than the combined effects of the Coulomb coupling of this electron to the $4f^6$ "core" electrons and spin-orbit coupling. In addition, evidence is found for the existence of a dynamical Jahn-Teller distortion of the orbitally degenerate e_g component of the $5d$ electron. The effects of the Jahn-Teller coupling on the ESR spectra of this excited state have features in common with the recently reported spectra of

other ions subject to dynamical Jahn-Teller interactions. We discuss the use of the line shape of the ESR spectrum to deduce the sign and magnitude of the Jahn-Teller distortion, and show that certain details of previous optical investigations of the Eu^{2+} ion can be explained as vibronic structure resulting from the Jahn-Teller distortion.

II. Eu^{2+} ION in CaF_2, SrF_2, and BaF_2

Numerous optical studies have been made on CaF_2: Eu^{2+}. The ground state is the cubic-field split $^8S_{7/2}$ level of the $4f^7$ configuration. The nearest excited levels are those of $4f^6 5d$, which leads to strong electric-dipole transitions with a sharp resonance line at 4130 Å and numerous lines and bands extending into the ultraviolet. In fluorescence at liquid-helium temperatures, the 4130-Å line is accompanied by vibronic sidebands extending to lower energies and peaking at about 4250 Å. The fluorescence spectrum of a 0.05% Eu^{2+} sample at 1.5 °K is shown in Fig. 1. It is evident that most of the fluorescence intensity is in the vibronic band, and the resonance line accounts for only about 2% of the total.

Measurements of the splitting of the 4130-Å line by applied stress[2] and magnetic field[3,4] show that the fluorescing level is a Γ_8 quartet. Two basically different models have been proposed to account for the behavior of the $4f^6 5d$ configuration. In one model, the level structure is considered as arising from the strong Coulomb coupling of the $5d$ electron to the $4f^6$ configuration to form ^3P_J multiplets, which are weakly split by tens of cm^{-1} in the cubic crystalline field. The evidence advanced in favor of this interpretation is the observed proportionality between the measured Faraday rotation[5] at frequencies far removed from the strong $4f$-$5d$ transitions and the magnetization of the $^8S_{7/2}$ ground state. This proportionality is only a necessary and not a sufficient condition that crystalline-field splittings are small in comparison with spin-orbit multiplet splittings. If the energy distributions of the oscillator strengths associated with transitions

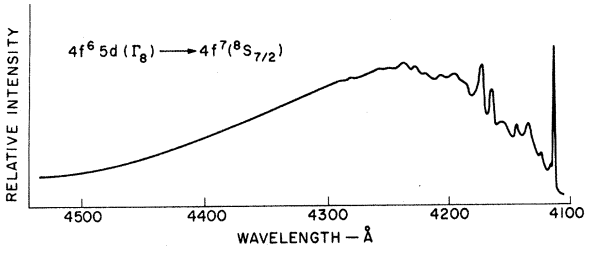

FIG. 1. Fluorescence spectrum of Eu^{2+} in CaF_2 at 4.2 °K.

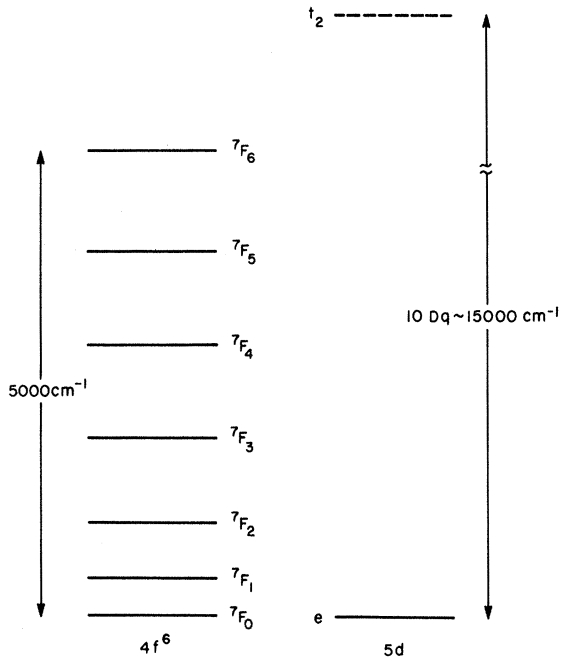

FIG. 2. Energy levels of the $4f^6$ and $5d$ configurations and their splittings due to spin-orbit coupling and cubic crystal field, respectively.

from the various Zeeman levels of $^8S_{7/2}$ are nearly the same, this proportionality will still exist and it is not clear that this will not be approximately true if the $5d$ electron undergoes a large crystal-field splitting.

There is, on the other hand, considerable evidence that the $5d$ electron is strongly split in the cubic field into its t_{2g} and e_g orbitals, the e_g being lowest. In all the spectra of $4f^{n-1}5d$ configurations, a pair of absorption bands is observed[6] separated by 10 000–20 000 cm^{-1}. This energy is most likely the 10 Dq splitting of the $5d$ electron. Estimates of the total electrostatic coupling between the $5d$ electron and the $4f^6$ configuration are the order of 7000 cm^{-1},[1] and the fraction of this coupling which would be effective in reducing the crystal-field splitting of the $5d$ electron might be considerably smaller than this. It is therefore natural to assume that the general scheme of the energy levels under these conditions is that shown in Fig. 2. The $^7F_0 \rightarrow {}^7F_6$ spin-orbit multiplets of the $4f^6$ core levels are coupled to the e and t_2 orbitals to produce a lowest-lying Γ_8 quartet, which should have many properties similar to those of a ^2E level in cubic symmetry. In fact, it has been noted that the behavior of the level when the lattice is subjected to external stress does conform to this description. However, because of the close spacing of the spin-orbit multi-

plets in the $4f^6$ configuration, its nominally $J=0$ ground state may be expected to be appreciably polarized in an external magnetic field by a coupling to the $5d$ electron spin of only a few hundred cm^{-1}. This will also seriously perturb the spacings of the multiplets, and will obviously have an appreciable influence on the magnetic properties of the metastable Γ_8 level.

The absorption and fluorescence spectra of the Eu^{2+} ion in SrF_2 are quite similar in character to those in CaF_2, except that the absorption and emission bands are shifted to higher energies. The absorption spectrum of BaF_2: Eu^{2+} has no zero-phonon transitions or other sharp structure as is found in CaF_2 and SrF_2. Furthermore, the Eu^{2+} fluorescence in this host does not appear to originate from the $4f^65d$ configuration because of the extremely large apparent Stokes shift of the fluorescence band,[7] which is several thousand cm^{-1} wide, structureless, and peaks at 5500–6000 Å. This fluorescence also disappears rapidly above 77 °K, and has a lifetime at 4.2 °K of about 10^{-4} sec, compared with $< 10^{-6}$ sec for the blue fluorescence in CaF_2 and SrF_2. It has been proposed[7] that these effects are due to an emitting level derived from the $4f^66s$ configuration of the Eu^{2+} ion. However, the quenching of the fluorescence above 77 °K suggests a thermal activation into a conduction-band state of the BaF_2 lattice. If this is true, the emitting state may be a trapped conduction electron at the resulting Eu^{3+} site, which is similar to the case of trivalent rare-earth dopants in semiconducting CdF_2.[8] The possibility that the $4f^65d$ levels may be in or above a conduction band in BaF_2 has been mentioned by Trautweiler *et al.*[9]

III. PARAMAGNETIC RESONANCE RESULTS

Electron-spin-resonance transitions were detected by the method of observing a circular polarization component of the entire fluorescent spectrum, resonance line plus vibronics, along the applied magnetic field.[10,11] Experiments were performed at 9.5 and 24 GHz. The data at 24 GHz had somewhat poorer signal to noise because of the difficulty in saturating the resonances with the available power of 250 mW. However, because of the large hyperfine splitting found for this level the 24-GHz results are far simpler to analyze. The general character of the resonances is similar to that of the ^2E level of Cr^{3+} and V^{2+} in MgO,[11] but in some respects it also resembles the spectra of MgO: Cu^{2+} [12] and CaF_2: Sc^{2+},[13] which have been characterized as having a moderate Jahn-Teller coupling and sizable tunneling splittings for the distorted configurations. We will return to this point later.

The resonance spectrum of Eu^{2+} in CaF_2 is summarized in Fig. 3. These traces were obtained with the sample immersed in liquid helium at 1.5 °K. The 3660-Å line of a 200-W high-pressure mercury-arc lamp was used to excite the Eu^{2+} fluorescence. A circular polarizer mounted inside the glass Dewar vessel and an ultraviolet cutoff filter preceded the *S*-20 photomultiplier which was used to detect the fluorescence. The microwaves incident on the cavity were chopped at 1 kHz, and the circularly polarized fluorescence propagating parallel to the external field was synchronously detected at this frequency. The fluorescence intensity was large enough to produce 10^{13} primary photoelectrons per second and led to a shot noise-limited sensitivity to signals about 10^{-7} of the total fluorescence. The signals in Fig. 3(a) result from a steady-state excited Eu^{2+} population of about 10^9.

In Fig. 3(a) spectra are shown for a magnetic field orientation along the crystalline [111] axis where the hyperfine components of the Eu^{151} and Eu^{153} isotopes, both having a nuclear spin $I=\frac{5}{2}$ and approximately equal abundance, are clearly resolved. As the field is rotated in a {110} plane, each line splits into two asymmetrically shaped components with sharp outside shoulders. This

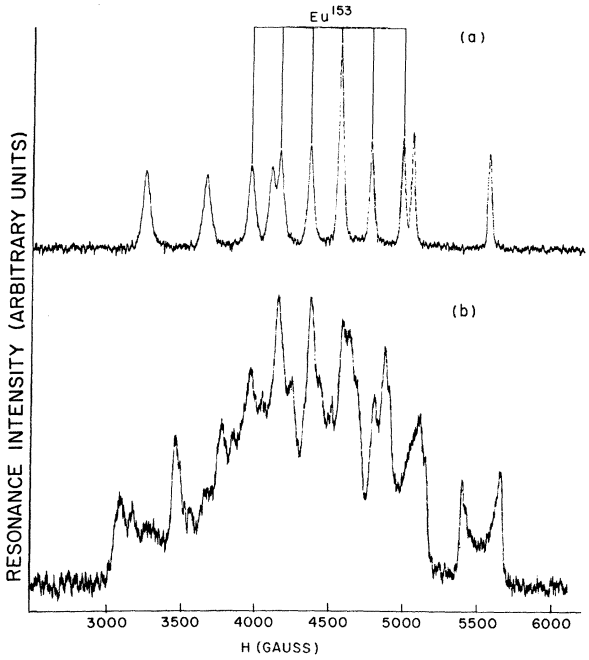

FIG. 3. Optically detected ESR signals for the metastable Γ_8 level of Eu^{2+} in CaF_2. The six hyperfine lines of Eu^{153} are marked in (a). The remaining five lines and the line overlapping with an Eu^{153} component are those of Eu^{151}. Field orientations are (a) along [111], (b) 15° from [111] toward a ⟨110⟩ axis.

effect is demonstrated in Fig. 3(b) in which the applied field is at 15° from [111] toward a ⟨100⟩ axis in the {110} plane. Only one of these shoulders remains observable for field orientations much further from [111]. This effect is discussed below.

At both 9.5 and 24 GHz, it was impossible to completely saturate the observed resonances with even 700 mW of microwave power incident on the cavity. Using the estimated cavity Q, the rotating field component at the sample is about 0.5 G. From this an upper limit on the T_1T_2 product is given by $g_1^2\beta^2H_1^2T_1T_2 \ll 1$ or $T_1T_2 < 3\times10^{-16}$ sec. As this estimate is exceedingly low, T_1 has been measured using pulse saturation at 9.50 GHz and direct observation of the recovery of the circular polarization signal using a sampling oscilloscope in series with a multichannel signal averager. The spin-polarization decay is exponential and gives $T_1 = 3.6\times10^{-7}$ sec at 1.5 °K. The decay rate is roughly linear in T up to 3 °K.

The shapes and anisotropy of the observed resonances are characteristic of those expected for an e_g orbital (or any ^2E level in a cubic field) if random-strain splittings of the orbital degeneracy are considered. This situation has been encountered previously in the ^2E level of Cr^{3+} in MgO [11] and has also been discussed recently by Ham. [14] If the random-strain splittings are neglected, the magnetic and hyperfine splittings of such a level are given by

$$E = g\beta H + Am_I\,,$$

$$g = g_1 \pm qg_2[1 - 3(l^2m^2 + l^2n^2 + m^2n^2)]^{1/2}, \qquad (1)$$

$$A = A_1 \pm qA_2[1 - 3(l^2m^2 + l^2n^2 + m^2n^2)]^{1/2},$$

where H is the applied magnetic field whose orientation is given by the direction cosines (l, m, n) relative to the cube axes, m_I is the component of nuclear spin along H, β is the Bohr magneton, and q is an orbital reduction factor resulting from vibronic coupling with the E_g vibrational modes of the fluorine ligands. Equation (1) predicts two resonances for each hyperfine component, symmetrically split about their average g value of g_1. This expression is an approximation to first order in g_2/g_1 and A_2/A_1. It is the terms in g_2 and $A2$ that split the orbital degeneracy of the level in absence of strain splittings. For the Γ_8 level of Eu^{2+}, this magnetic splitting is never greater than 0.15 cm^{-1} at a resonance frequency of 24 GHz. However, the random-strain splitting of this degeneracy is, on the average, several cm^{-1} and thus has a great influence on the resonance spectra. The random strains at a site are decomposed into e_θ and e_ε components where $e_\theta \sim (2z^2 - x^2 - y^2)$ and $e_\varepsilon \sim (x^2 - y^2)$ give their transformation properties. An angle φ is defined for each lattice site by $e_\varepsilon/e_\theta = \tan\varphi$, and it is assumed that the strain splitting of the orbital components at each lattice site is much greater than $g_2\beta H + A_2m_I$.

The resulting magnetic splitting of these strain-stabilized orbitals is then given by

$$g = g_1 \pm qg_2[\cos\varphi(3n^2 - 1) + \sqrt{3}\,\sin\varphi(l^2 - m^2)], \quad (2)$$

with an analogous expression for A. For a random-strain distribution, φ takes on values from 0 to 2π with equal probability, and the resulting resonance spectrum resembles a "powder pattern" with sharp boundaries at the positions of the zero-strain resonance components given by Eq. (2).

The observed resonances in Fig. (3) can be fit to such a spectrum for $g_1 = 3.68 \pm 0.01$, $gq_2 = 0.40 \pm 0.02$, $A_1 = 2360 \pm 30$ MHz, and $A_2 = 420 \pm 80$ MHz. These results have been corrected for second-order hyperfine shifts which are fairly large even at 24 GHz. The magnetic splitting of this level has also been measured using the Zeeman effect of the 4130-Å zero-phonon transition. [3,4] The results were fit to the more accurate expression [15]

$$g^2 = (5\gamma + 3\delta^2) \pm 4\gamma\{\gamma^2 + \tfrac{1}{2}\delta^2[l^4 + m^4 + n^4 - 3]\}^{1/2}. \quad (3)$$

The most recent Zeeman results [4] give $\delta^2 = 4.11 \pm 0.04$ and $\gamma^2 = 0.125 \pm 0.01$. The values obtained in this work are $\delta^2 = 4.43 \pm 0.02$ and $\gamma^2 = 0.045 \pm 0.005$.

The above values of g_1, g_2, A_1, and A_2 are obviously considerably different from those expected for a single $5d(e_g)$ orbital for which $g_1 \sim 2.1$, $g_2 \sim 0.1$, and $A_1 \sim 100$ MHz would be more reasonable. [16] However, it is not difficult to justify these results using a model in which an e_g orbital of a $5d$ electron interacts weakly (in comparison with its crystal-field splitting) with a $4f^6$ "core" having a $J = 0$ ground state. We assume a simple isotropic exchange coupling between the $5d$ and $4f$ spins

$$\mathcal{H} = 2\beta\vec{H}_{eff}\cdot\vec{S}_f\,,$$

where $\vec{S}_f$ is the total spin of the ^7F_J core levels. A computer diagonalization [17] of the five lowest ^7F_J multiplets in Fig. 2 has given the wave function for the ground state of $4f^6$ subject to this exchange coupling. The matrix element $\langle L_z + 2S_z\rangle$ calculated from this function is shown in Fig. 4 as a function of $\beta\vec{H}_{eff}/\lambda$ where $\lambda \sim 400$ cm^{-1} is the spin-orbit parameter for $4f^6$. The measured g_1 can be fit by values of $\langle L_z + 2S_z\rangle$ equal to $\frac{1}{2}(g_1 + 2) = 2.84$, opposing the $5d$ spin moment, and by $\frac{1}{2}(g_1 - 2) = 0.84$, if it adds to the $5d$ spin moment. The additive case can be ruled out on two counts: (i) The coupling in this case is $\beta H_{eff} \sim \frac{1}{4}\lambda = 100\ cm^{-1}$, which seems too small, and (ii) the hyperfine constant estimated for this situation is about 450 MHz, compared with the measured 2400 MHz. It is encouraging that $\langle L_z$

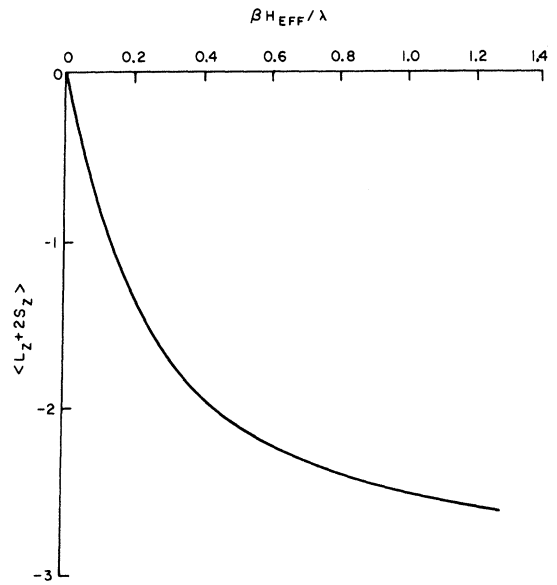

FIG. 4. The matrix element $\langle L_z+2S_z\rangle$ for the ground state of the $4f^6$ configuration subject to an effective exchange field. Crystal-field splittings of the $4f^6$ levels are neglected. Positive values are in the direction of H_{eff} in the text. The observed $g=3.68$ can be fit by values of $\langle L_z+2S_z\rangle$ of $\frac{1}{2}(g_1+2)=2.84$ and $\frac{1}{2}(g_1-2)=0.84$.

$+2S_z\rangle$ approaches $\frac{1}{2}(g_1+2)$ for $\beta H_{\text{eff}} \gtrsim \lambda$, and inclusion of the $^7F_5$ and $^7F_6$ levels may make the convergence more rapid. However, such a simple model of the $4f$-$5d$ coupling does not warrant further refinement. This result suggests that the $4f^6$ core levels of the $4f^6 5d$ configuration are appreciably altered by the f-d coupling and the many apparently successful attempts[2,6] to fit observed structures in the absorption spectrum of $CaF_2:Eu^{2+}$ to the spin-orbit multiplets of an Eu^{3+} core are fortuitous. Their success may result from assignment of vibronic features to electronic levels.

An alternative explanation of the large g factor and hyperfine coupling in the Γ_8 level is the admixture of another nearby configuration such as $4f^7$ into $4f^6 5d$ by lattice vibrational modes. Such a mechanism has been proposed[18] to explain anomalous vibronic spectra[19] for the Eu^{2+} $4f^7(^8S_{7/2}) \rightarrow 4f^5 5d$ transitions in alkali-halide lattices. To check on this possibility, we have examined the ESR spectra of the Γ_8 level in $SrF_2:Eu^{2+}$ and $BaF_2:Eu^{2+}$ at 24 GHz. The resonances in these lattices are much more difficult to saturate, and the signals are barely detectable even with the magnetic field along the [111] direction. For this reason, no detailed data were obtained for other field orientiations. The interesting result in these cases is that the g values and hyperfine-coupling constants for H along [111] are identical, within experimental error, to those of $CaF_2:Eu^{2+}$. This is interesting because the position of the Γ_8 level has shifted to higher energy in SrF_2 by about 700 cm^{-1}, and the resonances in BaF_2 were observed using the anomalous yellow fluorescence discussed above. No other resonances were observed in BaF_2 except for the ground-state resonances observed via the Faraday rotation of the yellow emission band. Thus, the ESR experiments yield no clue as to the nature of the emitting level in $BaF_2:Eu^{2+}$. It is probable that the observation of resonances characteristic of the $4f^6 5d$ level using this yellow fluorescence is indicative of a partial conservation of spin polarization in the radiationless decay from the $4f^6 5d$ level to the emitting level.

If vibrational coupling of a nearby level of $4f^7$ or $4f^6 6s$ is responsible for the large g shift and hyperfine interaction, it would be expected to yield at least slightly different spectra in SrF_2, BaF_2, and CaF_2 since the host-induced shifts of $4f^7$ and $4f^6 6s$ levels is unlikely to be identical to that of the $4f^6 5d$ levels. It appears most probable that the magnetic properties of the Γ_8 level are a result of the $4f$-$5d$ interaction discussed above.

An interesting effect, noticed in the Γ_8 resonance spectrum for magnetic field orientations far from [111], is summarized in Fig. 5 for large rotations toward [001] and [110] in a $\{1\bar{1}0\}$ plane. An asymmetric broadening of the split resonance compo-

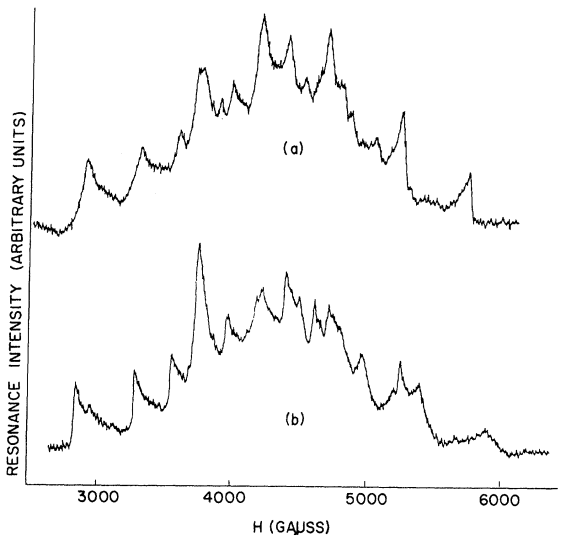

FIG. 5. Optically detected resonance spectra for Eu^{2+} in CaF_2 with the applied magnetic field at 25° from the [111] direction toward (a) [110] and (b) [001]. The broadening referred to in the text is most observable in the low-field components in (a) and the high-field components in (b).

nents occurs as $\vec{H}$ approaches [110]. The broadening of these components is approximately proportional to $|\Delta g(\theta)\beta H_0 + A(\theta)m_I)|$ to the first power. $A(\theta)$ and $\Delta g(\theta)$ are the anisotropic components of the g value and hyperfine constant [proportional to g_2 and A_2 in Eq. (1)] and θ is measured from the [001] axis. For a magnetic field orientation along [001], this broadening is so severe that the affected components cannot be detected at 24 GHz.

These effects can be correlated with the presence of a nearby "tunneling" state associated with the lattice coupling of the $5d$ electron, and Sec. IV discusses this coupling and direct spectroscopic evidence for the existence of such vibronic structure for Eu^{2+}.

IV. VIBRONIC COUPLING IN $4f^6 5d$ CONFIGURATION

The Γ_8 level of Eu^{2+} is not an ideal case for the study of vibronic interactions because of the complications resulting from the $4f$-$5d$ coupling. However, it is unique in that the sharp optical transition to this level appears to have structure due to the presence of a nearby Jahn-Teller tunneling state. A vibronic level of this type appears to be responsible for the unexplained observation by Kaplyanskii and Przevuskii[2] of an energy level in SrF_2: Eu^{2+} lying 6.5 cm^{-1} above the Γ_8 level. The optical transition to this level from the $^8S_{7/2}$ ground state is apparently highly forbidden in comparison with the transition to the Γ_8 level. However, under application of uniaxial strain to the sample, this level shifts and anticrosses with the split components of the Γ_8 level. If the applied stress contains a component of E symmetry, this is accompanied by a large increase in oscillator strength of the forbidden transition and a corresponding decrease in the oscillator strength of the $^8S_{7/2} \rightarrow \Gamma_8$ component. The form of this coupling to the Γ_8 level is illustrated in Fig. 6, which is obtained from Fig. 4 of Ref. 2. The shift of the nondegenerate level is identical to that of the Γ_8 level for both isotropic and trigonal strain components. The authors of Ref. 2 also report the existence of a similar level in CaF_2: Eu^{2+} about 15 cm^{-1} above the Γ_8 level, although no data are presented there because of the weakness of the anticrossing and borrowed intensity changes resulting from the greater separation of the levels.

The anticrossing and the changes of intensity of the electronic transition to this nearby level imply with reasonable certainty that it and the Γ_8 level are energy levels of the same ion. If this level is derived from another configuration of Eu^{2+} such as $4f^7$ or $4f^6 6s$, it is again difficult to understand why it should remain nearly coincident with the Γ_8 level in both CaF_2 and SrF_2 when the Γ_8 level has shifted by over 700 cm^{-1} relative to the ground state. If

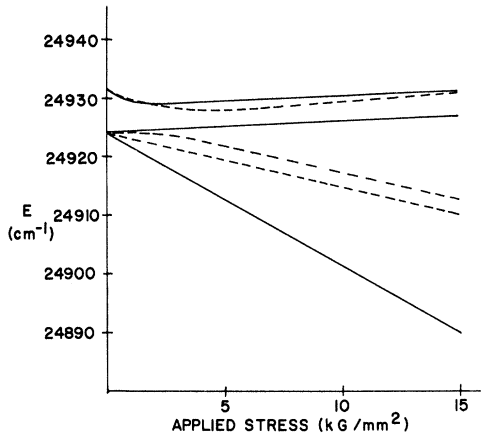

FIG. 6. Stress splitting and interaction of the E and A levels in CaF_2 obtained from Ref. 2. Full lines correspond to stress along [001], dotted lines to stress along [110]. Stress along a $\langle 111 \rangle$ axis leads to a uniform shift of E and A to lower frequencies with no splitting or interaction.

it is one of the higher-lying states of $4f^6 5d$, it is not clear why it should not also have an allowed electric-dipole transition to the ground state. We give here an alternative explanation for the existence of this level[20] which can explain all the observed features of the optical spectra and the selective broadening of the ESR components of the Γ_8 level.

Since the e orbital of the $5d$ electron is orbitally degenerate, it will interact with E-symmetry vibrational modes of the eight neighboring fluorine ions and this interaction leads to the Jahn-Teller effect in its many forms. Longuet-Higgins *et al.*[21] have examined the vibronic energy-level scheme for the case of linear Jahn-Teller coupling in a doubly degenerate level. This assumes an electron-lattice coupling of the form

$$\mathcal{H}' = \frac{1}{2\mu} \sum_k (\mu^2 \omega^2 Q_k^2 + P_k^2) + \sum_k V_{1k} Q_k \,, \qquad (4)$$

where Q_k is a coordinate of an E-symmetry vibration of the ligands and μ, ω, and P_k are its corresponding reduced mass, frequency, and generalized momentum. V_{1k} is the linear vibrational coupling coefficient. If plotted as a function of Q_k, this expression represents an effective potential surface on which the nuclei move and it is the well-known "Mexican hat",[14] shown in Fig. 7. In this figure, Q_2 and Q_3 are the degenerate E modes of the ligands transforming as

$$Q_2 \sim (x^2 - y^2), \quad Q_3 \sim (3z^2 - r^2) \,. \qquad (5)$$

The energy difference between the $Q_i = 0$ configuration and the minimum in the potential surface is

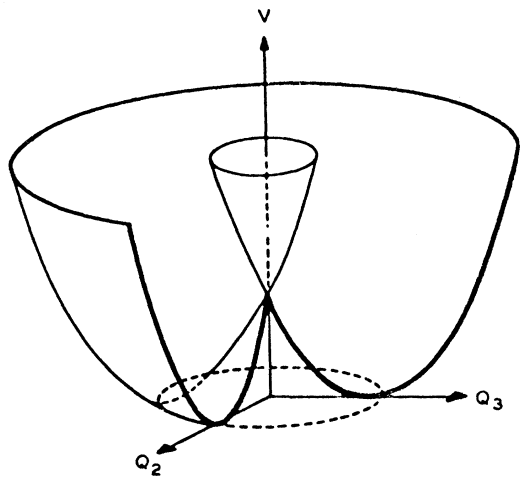

FIG. 7. Vibrational potential-energy surface resulting from the coupling of the e_g orbital of the $5d$ electron to the E-symmetry vibrational coordinates, $Q_2 = Q_\theta$ and $Q_3 = Q_\epsilon$ of the text.

$E_{JT} = V_{1k}^2/2\mu\omega$. If this is much larger than the zero-point vibrational energy of the E mode, the nuclear motion is confined at low temperatures to the lower portion of the potential surface such that

$$Q_2 = \rho_0 \sin\varphi, \quad Q_3 = \rho_0 \cos\varphi, \tag{6}$$

for $\rho_0 = |V_{1k}|/\mu\omega^2$.

Longuet-Higgins *et al.*[21] have shown that the nuclear Hamiltonian in this case is approximately separable into vibrational motion in ρ about the mean value ρ_0 and rotational motion in φ. They have obtained the eigenvalues for this problem and calculated matrix elements for electronic transitions to and from another nondegenerate electronic level. The nuclear wave functions in this strong coupling case are products of the form $u_m(\rho)e^{ij\phi}$, where the two lowest-lying energy levels have $j = \pm\frac{3}{2}$ and $j = \pm\frac{3}{2}$. The lower $j = \pm\frac{1}{2}$ level transforms as E in O_h and $j = \pm\frac{3}{2}$ as $A_2 + A_1$ states. These levels are separated by the amount[14]

$$\begin{aligned} \Delta E &\cong \hbar\omega[1 - 2E_{JT}/\hbar\omega] \quad \text{if } E_{JT} < \hbar\omega, \\ \Delta E &\cong (\hbar\omega)^2/2E_{JT} \qquad\quad \text{if } E_{JT} \gg \hbar\omega. \end{aligned} \tag{7}$$

For $E_{JT} \gg \hbar\omega$, then, these levels can be quite close in comparison with $\hbar\omega$. Child and Longuet-Higgins[22] and later Obrien[23] have included the effects of nonlinear electron-lattice coupling terms and anharmonic effects in Eq. (4), which introduce terms of the form

$$\mathcal{H}' = A_3 Q_3 (3Q_2^2 - Q_3^2) + V_2[Q_2^2 - Q_3^2 + 2Q_2 Q_3], \tag{8}$$

where A_3 represents the first-order anharmonicity of the E_g vibration and V_2 results from nonlinear coupling of the e_g orbital to the E_g vibration. The effect of these terms is to introduce φ-dependent "warping" in the surface of Fig. 7 with minima corresponding to tetragonal distortions along the cube axes. This warping is represented by an effective ionic potential for the fluorine ligands of the form

$$\mathcal{H}' = (V_2\rho^2 + A_3\rho^3)\cos 3\varphi \tag{9}$$

in the notation of Eq. (6).

This is accompanied by a mixing of the various rotational levels so that j modulo 3 is a good quantum number. These added terms also couple the two sheets of the potential surface in Fig. 7, an effect which is ignored here because it does not alter the qualitative features of the low-lying levels. These levels then correspond to those of a hindered rotator. The ground state remains a vibronically degenerate E level, but the $J = \pm\frac{3}{2}$ levels split into components transforming as A_1 and A_2. Which of these components lies lower is determined by the sign of the distortion stabilized by the terms in Eq. (9). In any case, the lower A level and E become degenerate as the combined effects of A_3 and V_2 in Eq. (9) increase. If the warping minima become substantially larger than the E_g vibrational mode energy, the model of a distortion tunneling between equivalent cube-axis minima becomes reasonable. The vibronic wave functions in this case are

$$\begin{aligned} \Psi(A) &= (3 - 6\gamma)^{-1/2}(\chi_x\Psi_x + \chi_y\Psi_y + \chi_z\Psi_z), \\ \Psi_\theta(E) &= (6 + 6\gamma)^{-1/2}(2\chi_z\Psi_z - \chi_x\Psi_x - \chi_y\Psi_y), \\ \Psi_\epsilon(E) &= (2 + 2\gamma)^{-1/2}(\chi_x\Psi_x - \chi_y\Psi_y), \end{aligned} \tag{10}$$

where χ_x is a vibrational wave function for the complex localized in a distortion along the x axis, Ψ_x is the e_g orbital stabilized by this distortion, and $\gamma = \langle\chi_x|\chi_y\rangle$, etc. In eightfold coordination, if the stable distortion is an elongation, A_1 lies lower and $\Psi_x \sim (2x^2 - r^2)$. If a compression is stabilized, A_2 lies lower and $\Psi_x = (y^2 - z^2)$, with obvious permutations for Ψ_y and Ψ_z. The residual splitting between E and the lowest A level is denoted 3Γ, and the θ and ϵ orbitals are referred to the z axis [001].

The first correlation between the A level in Eq. (12) and the additional level observed in Ref. 2 is that transitions to either A_1 or A_2 are forbidden at low temperatures in the absence of symmetry-lowering perturbations. This results from the fact that the A_1 and A_2 levels are orthogonal to the ground state of the original E_g vibrational mode, which is occupied in the $^8S_{7/2}$ ground state of Eu^{2+} at low temperatures. This rule holds rigorously for arbitrary values of A_3 and V_2 in Eq. (9).

If a uniaxial stress is applied to the crystal, the splitting of the E level and its coupling to A can be expressed in terms of the single reduced matrix element $V(E)$. The results are significantly different depending on whether A_1 or A_2 lies lowest and whether the tunneling model of Eq. (10) or a nearly free rotational model is correct for the vibronic levels. We summarize these results with the strain-tunneling matrix expressed in the notation of Ham[14]:

$$\begin{array}{c} \\ \Psi_\theta(E) \\ \Psi_\epsilon(E) \\ \Psi(A) \end{array} \begin{bmatrix} -qe(E_\theta)V(E) & & \\ qe(E_\epsilon)V(E) & qe(E_\theta) & \\ [re(E_\theta)+r'e(E_\epsilon)]\,V(E) & [r'e(E_\theta)+re(E_\epsilon)]\,V(E) & 3\Gamma \end{bmatrix} . \tag{11}$$

The diagonal elements of A_1 stress have been deleted, and the effects of T_2 (shear) stresses should be zero for an e_g orbital. We have used the normalized strain bases

$$e(E_\theta) = 2\epsilon_{zz} - \epsilon_{xx} - \epsilon_{yy}, \quad e(E_\epsilon) = \sqrt{3}\,(\epsilon_{xx} - \epsilon_{yy}).$$

In the tunneling limit, where the distorted configurations are well localized along the cube axes, r, r', and q may be calculated from the wave functions in Eq. (10). Assuming $\gamma \ll 1$, the results are (a) $r' = 0$, $r = \sqrt{2}\,q$, $q \sim \frac{1}{2}$ if A_1 is lowest and (b) $r' = \sqrt{2}q$, $r = 0$, $q \sim \frac{1}{2}$ if A_2 is lowest. In the opposite limit where the nonlinear terms are negligible compared to $\hbar\omega$, the wave functions are also simple and the above cases become (a) $r' = 0$, $r = q$, $q \sim \frac{1}{2}$, and (b) $r' = q$, $r = 0$, $q \sim \frac{1}{2}$. The orbital reduction factor q is identical to that in Eq. (1) for the anisotropic Zeeman splitting. Kaplyanskii and Przevuskii[2] have interpreted the results of their experiment on SrF_2: Eu^{2+} in terms of a phenomenological Hamiltonian resembling Eq. (11), although the strain experiment is not capable of determining the symmetry of the A level. We assume it is an A_1 level as has been proposed for the e_g orbital of $Sc^{2+}(3d')$ in CaF_2,[13] so that $r' \neq 0$. The most interesting result of the strain experiment is

$$(r'/q)_{\text{expt}} \equiv D/B = 1.40, \tag{12}$$

where D and B are parameters that were obtained in Ref. 2 from fits to the strain data. The scatter in the published data suggests an accuracy of 10% or so. This is in good agreement with the value $r'/q = \sqrt{2}$ expected for the tunneling model. Similar measurements were not reported[2] for the CaF_2 lattice, presumably because 3Γ is much larger and the strain coupling to the E level is difficult to observe.

We now turn to the explanation of the orientational-dependent linewidths of the ESR spectrum in CaF_2 and show how these may be explained by the existence of such a tunneling level at about 15 cm^{-1} in this case, as observed in Ref. 2. When the applied magnetic field lies in a $\{1\bar{1}0\}$ plane, the vibronic functions which diagonalize the Zeeman Hamiltonian are $\Psi_\theta(E)$ and $\Psi_\epsilon(E)$ in % (10) where Ψ_z is quantized along the $\langle 001\rangle$ axis lying in the $\{1\bar{1}0\}$ plane. When the resonances are "washed out" by random strain, the sharp edges of the spectrum correspond to resonance transitions at those sites having a predominantly E_θ symmetry strain quantized along [001], since this is diagonal in $\Psi_\theta(E)$ and $\Psi_\epsilon(E)$.

There exist matrix elements of the anisotropic components of the Zeeman Hamiltonian coupling the states of the E level to the tunneling level. It is the combination of the random-strain coupling and the Zeeman coupling to the tunneling level in this case which broadens the resonance components selectively as illustrated in Fig. 5.

The relevant perturbation expression is of the type

$$\mathcal{H}' = \langle \Psi_\theta(E)\,|e(E_\theta)|\,\Psi(A_1)\rangle\langle\Psi(A_1)|\mathcal{H}_Z|\,\Psi_\theta(E)\rangle\,/3\Gamma\,, \tag{13}$$

where $e(E_\theta)$ is the (predominant) component of random strain at a site whose resonances appear at the sharp edges of the spectrum and $\mathcal{H}_Z$ is the Zeeman Hamiltonian. The corresponding expression involving the orbital state $\Psi_\epsilon(E)$ is zero because $e(E_\epsilon)$ does not couple this state to $\Psi(A_1)$ as is evident from the above strain-tunneling matrix. This explains why the broadening affects only one orbital component of the resonance spectrum if it is assumed that the $\Psi_\theta(E)$ resonance is at the high-field edge for $\vec{H}$ along [001] and at the low-field edge when $\vec{H}$ is along [110]. If the overlap factor γ is assumed negligible compared with unity, this broadening can be related approximately to the tunneling splitting 3Γ by computing the matrix elements in Eq. (11) and the result is

$$\Delta H(\theta) \sim \bar{\delta}[\Delta g(\theta)\beta H + A_2(\theta)]/3\Gamma g\beta\,, \tag{14}$$

where $\bar{\delta}$ is the mean random-strain splitting of the E level and $\Delta g(\theta)$ and $A_2(\theta)$ are the measured anisotropic components of the magnetic splitting given by Eqs. (2) and (3). We have performed a more accurate analysis of these effects by computer

diagonalization of Eq. (11) assuming a Gaussian strain distribution $P(\delta) \propto \exp(-\delta^2/2\bar{\delta}^2)$ and a uniform probability distribution for $\Phi = \tan^{-1}(e_\epsilon/e_\theta)$, $0 \leq \Phi < 2\pi$. The magnetic splittings of the resulting sets of three Kramers doublets were then calculated as a perturbation assuming $\gamma = 0$. Matrix elements of the magnetic interaction coupling different doublets were ignored since $\Delta g\beta H \ll \bar{\delta}$. The line shapes observed for the E level of Eu^{2+} in CaF_2 were then fitted by the ratio $\bar{\delta}/3\Gamma = 0.17$. $\bar{\delta}$ may be estimated in this case from the observed width of the optical transition to the E level, which can be corrected for coupling to A_1 strains using the data of Ref. 2. This gives $\bar{\delta} \sim 3$ cm^{-1} and $3\Gamma \simeq 18 \pm 4$ cm^{-1}. This is in good agreement with the stress-optical[2] observations of a level at 15 cm^{-1}, and supports the conclusion that the optical experiments of Ref. 2 are indeed explained in terms of tunneling excitations.

The calculated line shapes for this strain-tunneling competition show effects which may be of interest to other cases of ESR spectra of Jahn-Teller distorted ions.

The results are summarized in Fig. 8 which gives the resonance line shapes as a function of $\bar{\delta}/3\Gamma$, the ratio of the mean strain splitting to the tunneling splitting. Thermalization at a temperature $kT = 0.5\bar{\delta}$ was assumed which accounts for the absence of the isotropic line at g_1 for the singlet excited level in the region $3\Gamma \gg \bar{\delta}$. It is apparent from these curves that the broadening effects which we are observing in the E level of Eu^{2+} are simply the beginning of the random-strain-induced transition to a "static" Jahn-Teller spectrum. When $\bar{\delta} \gg 3\Gamma$, the broadened edge of the resonance spectrum becomes sharp again at a new position characteristic of an axial spectrum with $g_\parallel = g_1 \pm g_2$, $g_\perp = g_1 \mp \frac{1}{2}g_2$, depending on the sign of the stabilized distortion. For a field orientation along [110], curves similar to those of Fig. 8 are obtained with the high-field component broadened and shifted, as expected. At field orientations not in the (110) plane, both edges of the tunneling resonances broaden as $\bar{\delta}/3\Gamma$ increases, and the spectrum condenses into three sharp lines characteristic of the three stable axial distortions. It is apparent that when dealing with spectra of Jahn-Teller perturbed levels, the detailed line shape, much of which is lost by field modulation techniques, is of great importance in determining the parameters of the Jahn-Teller coupling. In particular, we have noticed that (1) in the limit $3\Gamma \gg \bar{\delta}$, the relative heights of the "powder pattern" peaks are sensitive to 3Γ, even when $3\Gamma = 100\bar{\delta}$. (2) In the opposite limit $3\Gamma \ll \delta$ the relative heights of the parallel and perpendicular lines in Fig. 7(f) deviate by several percent from the expected ratio of 2:1 for $\bar{\delta} = 300\Gamma$. (This ratio must also be corrected to account for the different transition moments.) Although both these effects are influenced by the ratio of residual linewidth ΔH to the total magnetic anisotropy, the conditions used in these computations were $\frac{3}{2}g_2\beta H \sim 100\Delta H$. Such sharp lines are observed in the static spectra of Cu^{2+} in deuterated water crystals, for which attempts to determine 3Γ by spin-echo techniques led to ambiguous results.[24] It is possible that careful measurements of relative resonance intensities will resolve the problem. As an aid in planning such experiments, the computer-calculated ratio of intensities of the "parallel" and "perpendicular" resonance lines is plotted in Fig. 9 as a function of $3\Gamma\sqrt{\delta}$. Again, we note that off-diagonal perturbations of the Zeeman Hamiltonian have been neglected in this calculation and will have to be considered when they become comparable with 3Γ.

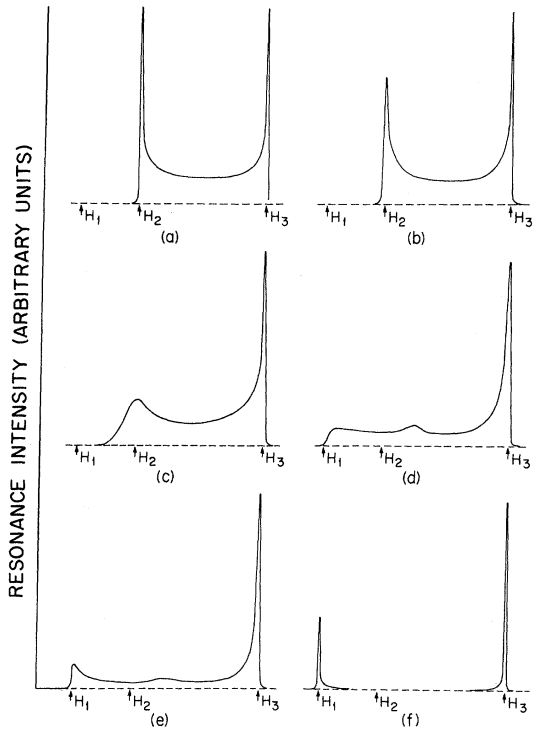

FIG. 8. ESR line shapes calculated for an external field applied along a (001) axis for various ratios of random-strain splitting to tunneling splitting ($\bar{\delta}/3\Gamma$). (a) $\bar{\delta}/3\Gamma = 0$, (b) $\bar{\delta}/3\Gamma = 0.01$, (c) $\bar{\delta}/3\Gamma = 0.1$, (d) $\bar{\delta}/3\Gamma = 0.5$, (e) $\bar{\delta}/3\Gamma = 1.0$, (f) $\bar{\delta}/3\Gamma = 10.0$. $H_1 = h\nu/(g_1 + g_2)\beta$, $H_2 = h\nu/(g_1 + \frac{1}{2}g_2)\beta$, and $H_3 = h\nu/(g_1 - \frac{1}{2}g_2)\beta$.

Ham has proposed[14] that uniaxial stress-splitting measurements on the E level can be used to deduce the strength of the vibronic coupling. He calculated the E_g mode distortion amplitude of the nearest neighbors in sixfold or eightfold coordination in terms of the macroscopic E_g symmetry strains

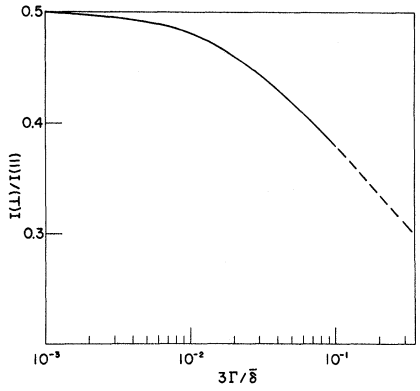

FIG. 9. Ratio of the intensities of the resonances due to complexes distorted along axes perpendicular and parallel to the applied magnetic field (which is assumed to be along a cube axis) as a function of $3\Gamma/\bar{\delta}$.

used in Eq. (11). For the case of eightfold coordination, the results are

$$V_{1k}=3V(E)/4R,\quad E_{JT}=9[V(E)]^2/32\mu\omega^2R^2\ , \qquad (15)$$

where V_{1k} is the linear strain coefficient in Eq. (4), R is the ion-ligand separation, and $V(E)$ is the reduced matrix element in Eq. (4). From the strain data,[2] we obtain $qV(E)=1.37\times10^4$ cm^{-1} for SrF_2. We have used the 4.2 °K elastic constants measured for CaF_2 and SrF_2 to obtain these results. The existence of excited vibronic levels at about 10 cm^{-1} is sufficient justification to assume $q=\frac{1}{2}$ to obtain $V(E)$.[14]

It is clear from Eqs. (7) and (15) that the position of the first excited level in the limit $E_{JT}\gtrsim\hbar\omega$ is proportional to $(\hbar\omega)^4$ where ω is an effective frequency for the mode or modes to which the e_g orbital couples. Thus, the choice of an effective mode frequency is rather critical, especially in this case where a sizable Stokes shift in absorption and fluorescence could be accompanied by a change in force constants for E_g distortions in the excited state. A point-charge calculation has recently yielded a set of dispersion curves and density of states for CaF_2.[25] The lowest-frequency peak in the state density which appears to have a substantial E_g component at the calcium site is at about 250 cm^{-1}. Another peak at 175 cm^{-1} would seem to have little E_g component since it arises from TO and TA modes having odd parity in this frequency region. The use of a 250-cm^{-1} effective frequency does give a reasonable agreement with the position of the tunneling levels in CaF_2 and SrF_2. To illustrate this and the sensitivity of the spacing of the E and A levels to the mode frequency, we have summarized in Table I the values of E_{JT} calculated from Eq. (15), the spacing ΔE of E and A for linear coupling only, and the magnitude of $\mathcal{K}'$ estimated from O'Brien's curves[23] to reproduce the measured spacing of $3\Gamma=6.8$ cm^{-1} for SrF_2 as a function of effective mode frequency. Since we know from the form of the strain splitting that the SrF_2:Eu^{2+} is near the tunneling limit, we must have $(V_3\rho_0^3+A_2\rho_0^2)\gtrsim\frac{1}{2}\hbar\omega$. On this basis, a $\hbar\omega$ of between 250 and 300 cm^{-1} seems most reasonable since higher frequencies lead to nonlinear effects comparable with E_{JT}. The relatively large difference in 3Γ for CaF_2 and SrF_2 can easily arise from a slight increase in ω as is evident from Table I. The only conclusion which can be reached regarding the use of uniaxial strain measurements to estimate the strength of the Jahn-Teller coupling is that it leads to reasonable results in this case.

V. SUMMARY AND CONCLUSIONS

The results of our ESR investigation of the emitting level of Eu^{2+} support the model of a large crystal-field splitting of the $5d$ electron and a $4f^6$-$5d$ exchange coupling which is at least comparable with the spin-orbit coupling parameter $\lambda\cong400$ cm^{-1} for the ^7F_J multiplets of $4f^6$. The resonance data and the results of the stress-optical experiments of Ref. 2 are consistent with a dynamical Jahn-Teller distortion of the e_g orbital of the $5d$ electron with $E_{JT}\sim10^3$ cm^{-1}, and the vibronic level at ~10 cm^{-1} above the E level in CaF_2, and SrF_2 appears to have vibronic wave functions characteristic of the tunneling limit. Both of these conclusions are consistent with the magnitude of the splitting of the E level by applied uniaxial strain if it is assumed that the E_g distortions at an Eu^{2+} site are characterized by a single oscillator with a frequency near to that of a density-of-states peak in the optic modes of the host lattice.

The use of the detailed shapes of the ESR spectra may have application to several other ions having Jahn-Teller interactions. The sign of the distortion

TABLE I. Jahn-Teller coupling parameters obtained from the measured uniaxial strain and tunneling splittings for the Γ_8 level of Eu^{2+} in SrF_2 for several E_g vibration frequencies. ΔE is the expected "rotational" splitting of the $j=\pm\frac{1}{2}$ and $j=\pm\frac{3}{2}$ states if V_3 and A_2 were zero.

$\hbar\omega$ (cm^{-1})	E_{JT} (cm^{-1})	ΔE (For linear coupling only) (cm^{-1})	$(V_3\rho_0^3+A_2\rho_0^2)$ (cm^{-1})
150	3300	3.5	···
200	1900	11	15
250	1200	26	80
300	700	75	~350
350	620	100	>400

stabilized by the nonlinear coupling terms in Eq. (9) as well as an estimate of the position of the nearest excited vibronic level can be obtained from these shapes. Of greater utility to the study of Jahn-Teller distortions would be the effects of applied stress on the ESR spectrum. From studies of relative intensity changes of the resonances of the two vibronic components due to thermalization at low temperatures, the stress coupling coefficient can be obtained. Observation of the positions of the resonances as a function of strain can then be used to extract the position of the excited vibronic level and its coupling to the ground state by applied strain. No complete study of this type has been done as yet.

The absence of any resonances characteristic of the emitting level of Eu^{2+} in the BaF_2 lattice is puzzling. The observation of the $4f^6 5d$ resonances proves that the spin-lattice relaxation time in this state is not too fast compared with the 10^{-4}-sec fluorescence lifetime that all spin polarization is destroyed before emission occurs. It is also clear that the selection rules for the radiative transition to the ground state allow the detection of spin polarization in the excited state. A possible explanation would be that this emitting level has appreciable $6s$ character and the resulting contact hyperfine interaction with the large Eu^{151} and Eu^{153} nuclear moments places these resonances outside the 24-GHz frequency region for applied fields up to 17 kG, which were employed in these experiments.

ACKNOWLEDGMENTS

The author is grateful to Dr. S. Geschwind, Dr. F.S. Ham, and Dr. M.D. Sturge for helpful discussions, to Mrs. R.C. Fulton for assistance with numerical computations and to J. L. Davis for technical assistance.

---

*Present address: Physics Department, Indiana University, Bloomington, Ind.

[1]D. S. MCclure and Z. Kiss, J. Chem. Phys. 39, 3251 (1963).

[2]A. A. Kaplyanskii and A. K. Przevuskii, Opt. i Spektroskopiya 19, 597 (1965) [Opt. Spectry. (USSR) 19, 331 (1965)].

[3]B. P. Zakharchenya and I. B. Rusanov, Opt. i Spektroskopiya 18, 999 (1965) [Opt. Spectry. (USSR) 18, 563 (1965)].

[4]P. Kisliuk, H. H. Tippins, C. A. Moore, and S. A. Pollack, Phys. Rev. 171, 336 (1968).

[5]Y. R. Shen and N. Bloembergen, Phys. Rev. 133, A515 (1963); Y. R. Shen, *ibid.* 134, A661 (1964).

[6]E. Loh, Phys. Rev. 175, 533 (1968).

[7]A. A. Kaplyanskii and P. P. Feofilov, Opt. Spektroskopiya 13, 235 (1965) [Opt. Spectry. (USSR) 13, 129 (1962)].

[8]P. Eisenberger, P. S. Pershan, and D. R. Bosomworth, Phys. Rev. Letters 21, 543 (1968).

[9]F. Trautweiler, F. Moser, and P. R. Khasla, J. Phys. Chem. Solids 29, 1869 (1968).

[10]G. F. Imbusch and S. Geschwind, Phys. Letters 18, 109 (1965).

[11]L. L. Chase, Phys. Rev. 168, 341 (1968).

[12]R. E. Coffman, J. Chem. Phys. 48, 609 (1968).

[13]U. T. Hochli, Phys. Rev. 162, 262 (1968).

[14]F. S. Ham, Phys. Rev. 166, 307 (1968).

[15]B. Bleaney, Proc. Phys. Soc. (London) 73, 937 (1969).

[16]W. Hayes and J. W. Twidell, Proc. Phys. Soc. (London) 82, 330 (1963).

[17]We are grateful to H. W. de Wijn for the use of his computer program.

[18]W. E. Bron and M. Wagner, Phys. Rev. 145, 689 (1966).

[19]W. E. Bron and W. R. Heller, Phys. Rev. 136, A1433 (1964).

[20]L. L. Chase, Phys. Rev. Letters 23, 275 (1969).

[21]H. C. Longuet-Higgins, U. Opik, M. H. L. Pryce, and R. A. Sack, Proc. Roy. Soc. (London) 244A, 1 (1958).

[22]M. S. Child and H. C. Longuet-Higgins, Phil. Trans. Roy. Soc. London 254, 259 (1961).

[23]M. C. M. Obrien, Proc. Roy. Soc. (London) A281, 323 (1964).

[24]D. P. Breen, D. C. Krupka, and F. I. B. Williams, Phys. Rev. 179, 241 (1969).

[25]P. Eisenberger (private communication).